journal

J. Am. Ceram. Soc., 72 [5] 775-80 (1989)

Processing of Boron Carbide–Aluminum Composites

Danny C. Halverson*

Lawrence Livermore National Laboratory, University of California, Livermore, California 94550

Aleksander J. Pyzik* and Ilhan A. Aksay*

Department of Materials Science and Engineering, University of Washington, Seattle, Washington 98195

William E. Snowden*,*

Lawrence Livermore National Laboratory, University of California, Livermore, California 94550

The processing problems associated with boron carbide and the limitations of its mechanical properties can be significantly reduced when a metal phase (e.g., aluminum) is added. Lower densification temperatures and higher fracture toughness will result. Based on fundamental capillarity thermodynamics, reaction thermodynamics, and densification kinetics, we have established reliable criteria for fabricating B_4C–Al particulate composites. Because chemical reactions cannot be eliminated, it is necessary to process B_4C–Al by rapidly heating to near 1200°C (to ensure wetting) and subsequently heat-treating below 1200°C (for microstructural development). [Key words: composites, boron carbide, aluminum, processing, cermets.]

I. Introduction

BORON CARBIDE (B_4C)† is a very hard (9.5+ in Mohs scale),[1] low specific gravity (2.52), covalent ceramic that offers distinct advantages for applications involving neutron absorption, wear resistance, and impact resistance. The extreme sensitivity of B_4C to brittle fracture (K_{Ic} = 3.7 MPa · $m^{1/2}$)[2] and the difficulties associated with fabricating fully dense microstructures are serious limitations, however. By using certain additives (e.g., graphite), B_4C sintered at high temperatures (>2000°C) can produce microstructures with a high density (≈98.2% of theoretical density).[3] Full density is usually achieved through costly hot-pressing techniques;[4] however, even in a fully dense form, the sensitivity of boron carbide to brittle fracture remains a major limitation.

Our experiments demonstrated that the processing problems and mechanical property limitations associated with B_4C ceramics can be significantly reduced by introducing a metal phase (i.e., by developing B_4C cermets). If the application is limited to low temperatures, then a low-melting-point metal phase (e.g., aluminum or aluminum alloys) can be introduced to obtain lower densification temperatures (<1200°C) and to increase fracture toughness many times that of B_4C. In addition, if the metal phase has a low specific gravity, then the resulting cermet can have improved mechanical properties with low weight.

High-strength (>1000 MPa) B-C-Al composites consisting of B_4C-coated boron fibers in an aluminum matrix (≈50 vol% ceramic) have been fabricated.[5] Particulate B_4C–metal composites currently manufactured include materials consisting of dispersion-hardened metals (≤25 vol% B_4C),[1,6] boral (30 to 50 vol% B_4C),[7] and B_4C–Cu cermets (≈60 vol% B_4C).[8] In these composites, processing temperatures are kept to a minimum (<1000°C), primarily to avoid chemical reactions between B_4C and the metal phase.

In our work with particulate B_4C–Al composites which have a greater ceramic content (>55 vol%), we employed processing temperatures above 1000°C to promote wetting and to permit carefully controlled reactions in the system. Wetting is necessary to achieve strong interfacial bonding and to allow liquid rearrangement during sintering. If wetting does not occur, external pressure must be applied to improve consolidation; however, even pressure techniques are not satisfactory for densification of some high-ceramic-containing (>60 vol%) composites.[8]

We illustrate in this paper the importance of achieving a wetting condition in the processing of high ceramic content (>55 vol%), particulate-based B_4C–Al composites, the importance of understanding the phase equilibria in the B-C-Al system for the microstructural design of these cermets, and appropriate processing methods for producing cermets with negligible porosity.

II. Processing Experiments

(1) *Materials and Specimen Preparation*

We used sessile drops formed from high-purity aluminum shot (99.999% pure), hot-pressed B_4C substrates made from commercial-grade B_4C powders, and B_4C–Al compacts made from commercial-grade B_4C and aluminum powders. Compacts were small, generally 2.54 cm in diameter and 0.32 to 0.64 cm thick.

To prepare these compacts, we mixed B_4C powder§ (three particle-size distributions with median sizes of 4, 10, and 56 μm) and aluminum powder¶ (−325 mesh) in isopropyl alcohol, ultrasonically mixed the slurry to achieve homogeneity, and consolidated the solids by filtration in a plaster-of-Paris mold. These compacts were too weak for handling purposes; therefore, the composite powders were subsequently cold-pressed at 138 MPa (≈20 000 psi). We found that higher pressures resulted in undesirable striations in the compacts.

(2) *Procedures*

Our processing experiments included contact-angle measurements, chemical reaction studies, and densification studies in the molten aluminum–B_4C system.

In conducting our contact-angles experiments, we placed alu-

J. J. Petrovic—contributing editor

Manuscript No. 199146. Received November 19, 1986; approved September 2, 1988.

Supported by the U.S. Department of Energy at Lawrence Livermore National Laboratory under Contract No. W-7504-ENG-48 and by the U.S. Air Force Office of Scientific Research under Grant No. AFOSR-83-0375 at the University of Washington.

*Member, American Ceramic Society.

*Now with the Office of the Director of Defense Research and Engineering, The Pentagon, Washington, DC 20301.

†B_4C herein refers to the complete homogeneous range of compositions for boron carbide.

§ESK, GmbH, Munchen, FRG.

¶Alfa Products, Danvers, MA.

Table I. Vacuum-Hot-Pressed B_4C–Al Densification Results*

Aluminum content (vol%)	B_4C grain size (μm)	Maximum temperature (°C)	Indicated pressure (MPa)	Residual compact porosity (vol%)
30	<2	1180	15	24
50	<2	1180	15	8
50	<2	1050	20	14
50	<20	1150	15	22
60	<20	1100	15	13

*All runs took 75 min to reach maximum temperature. Maximum temperature hold time was 6 min at the indicated pressure with pressure being applied after passing through 800°C. Processing environment was $\approx 5 \times 10^{-2}$ Pa (10^{-3} to 10^{-4} torr). Samples were furnace cooled in vacuum under the indicated pressure. Porosity was determined by bulk density measurements.

Table II. Hot Isostatic Pressed B_4C–Al Densification Results*

Aluminum content (vol%)	B_4C average grain size (μm)	Maximum temperature (°C)	Sample presintered†	Residual connected porosity (vol%)
15	55	1000	Yes	3.50
30	55	1000	Yes	0.11
45	55	1000	Yes	0.04
30	4	750	No	>10

*All samples were run at the maximum temperature with a 30-min hold at 207-MPa argon. Heating and cooling rates of 50°C/min were used at 207 MPa. Porosity was determined by immersion density measurements after 5 min. †1180°C for 2 min at $\approx 10^{-3}$ Pa.

minum sessile drops on hot-pressed B_4C substrates (polished to a 1-μm finish) and heated them in a tungsten-mesh, resistance-heated vacuum furnace at pressures less than 5×10^{-3} Pa but greater than 10^{-4} Pa (typically between 10^{-5} and 10^{-6} torr). After the specimens were vacuum cooled to room temperature and taken out of the furnace, we measured the contact angles to within 1° using a protractor grid and optical 10× telemicroscope.

To investigate the nature and extent of the chemical reactions at the B_4C–Al interface, we examined polished (1-μm finish) cross sections of specimens from the wetting experiments using both optical and scanning electron microscopes. Further studies included X-ray diffraction (XRD), energy dispersive spectroscopy, and electron microprobe analyses to identify the reaction products in the microstructures of the sintered compacts.

In our densification kinetics studies, we subjected the B_4C–Al powder compacts to pressureless sintering, hot-pressing, and hot isostatic pressing. We sintered specimens in the tungsten-mesh, resistance-heated vacuum furnace at the same pressures used in the sessile-drop experiments. Hot-pressing and hot isostatic pressing were performed in accordance with the processing information in Tables I and II. Some hot isostatically pressed samples were presintered because they were processed at temperatures lower than those required for adequate wetting. To determine the level of residual porosity, we made immersion density** and bulk density measurements on each compact.

Weight loss due to evaporation of aluminum was not measured. Weight loss was evident, however, because furnace contamination was observed. Weight-loss measurements would be difficult because many phases are forming with different theoretical densities.

**Model 200 (2.0 centistrokes), Dow Corning Corp., Midland, MI.

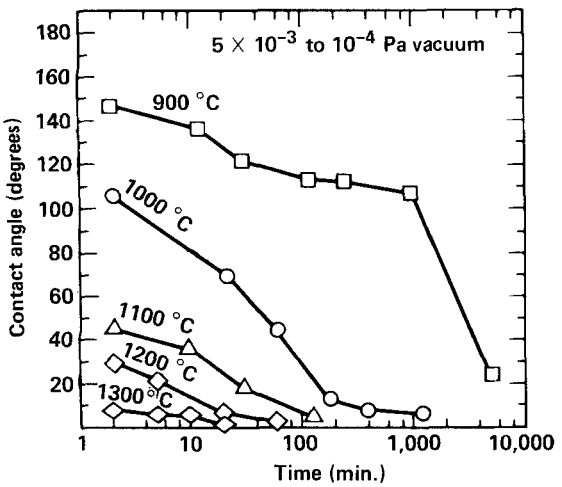

Fig. 1. Contact angle of molten aluminum on B_4C as a function of processing time for various isotherms at 5×10^{-3} to 1×10^{-4} Pa. Measurements were obtained after sessile drop was furnace cooled to room temperature.

III. Results and Discussion

(1) Wetting

An important point to be realized is that a nonwetting system can be transformed to a wetting system by taking advantage of chemical reactions.[9] Previous studies on the B_4C–Al system did not correctly recognize this fact, and, as a result, both obtuse[10,11] and acute[11–14] contact angles were reported as equilibrium values. Previous works[10,15] on B_4C–Al composites were discontinued when it was concluded that aluminum did not wet B_4C.

Figure 1 shows the contact angle of aluminum on B_4C as a function of temperature and time. Based on our contact-angle data, processing of B_4C–Al composites below 1000°C cannot be accomplished by pressureless sintering techniques because acute contact angles are not obtained in reasonably short times. By increasing the temperature, low contact angles are obtained in reasonably short times; however, because the vapor pressure of aluminum also increases with increasing temperature, an upper processing temperature limit is also necessary to keep vaporization of the aluminum to a minimum.

The dynamic nature of the contact angle of aluminum on B_4C is associated with the mass transfer across the solid–liquid interface as the system moves toward a state of chemical equilibrium. During this dynamic stage, the contact angle cannot be expected to remain constant because the interfacial tensions between the solid, liquid, and vapor phases will be continuously changing as a result of compositional and structural variations across the interfaces. The nature of these reactions will be discussed in the next section.

(2) Reaction Thermodynamics

At least nine ternary phases have been reported for the B-C-Al system;[16–28] consequently, it is important to select processing conditions that will allow only certain reaction products to form so that desired properties (negligible Al_4C_3) will be obtained. Previous attempts[29] to fabricate B_4C–Al cermets were discontinued when it was concluded that the reaction products were detrimental to mechanical properties.

We investigated the reaction products that occur under different sets of wetting conditions. Figure 2 illustrates the results of our reaction thermodynamic studies from 800° to 1400°C and the reaction products that form when local equilibrium conditions are achieved. Under these conditions, sufficient aluminum is present to sustain the reactions shown. For any starting composition, the initial reaction products will always form at the expense of B_4C and aluminum.

Figure 3 shows some of the characteristic microstructures that can be obtained under conditions of local equilibrium. An unidentified phase, called phase X, forms at all of the temperatures in this study. Phase X can coexist with B_4C. Initial attempts to identify phase X were unsuccessful because its XRD pattern did not match any binary Al_xB_y, Al_xC_y, B_xC_y; ternary $Al_xB_yC_z$; or binary or ternary oxide, nitride, oxycarbide, oxynitride, or car-

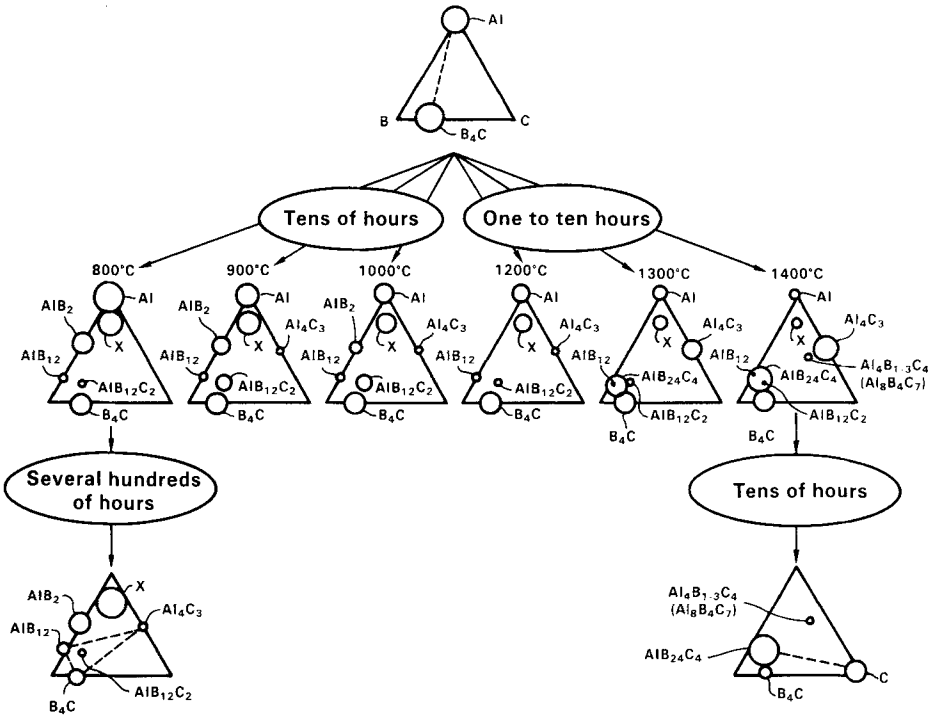

Fig. 2. Thermodynamic-reaction-series map for B_4C–Al composites initially densified at 1180°C and heat-treated under various isothermal conditions between 800° and 1400°C.

bonitride XRD patterns.[30] Some of the characteristic XRD lines for phase X have been recently reported,[31] and energy dispersive X-ray and electron microprobe analyses indicate that phase X is largely aluminum with smaller amounts of boron and carbon.

In a recent study, Sarikaya *et al.*[32] characterized the crystal structure and composition of phase X by transmission electron microscopy techniques. Electron diffraction studies indicate that the crystal structure of phase X is hexagonal close packed with lattice parameters quite different from any of the other binary or ternary phases in the B-C-Al system. Their preliminary studies by electron energy loss spectroscopy indicate that the composition of phase X is Al_4BC.

B_4C and aluminum react to form phase X. Under local equilibrium between 800° and 900°C, AlB_2 and phase X are the major reaction products. Under these conditions, phase X is stable, and it will decompose only after all of the free aluminum is depleted from the system. Above 1100°C, there is less phase X because aluminum is rapidly being depleted through the formation of other more thermodynamically stable phases.

Figure 3(A) shows a typical microstructure in local equilibrium

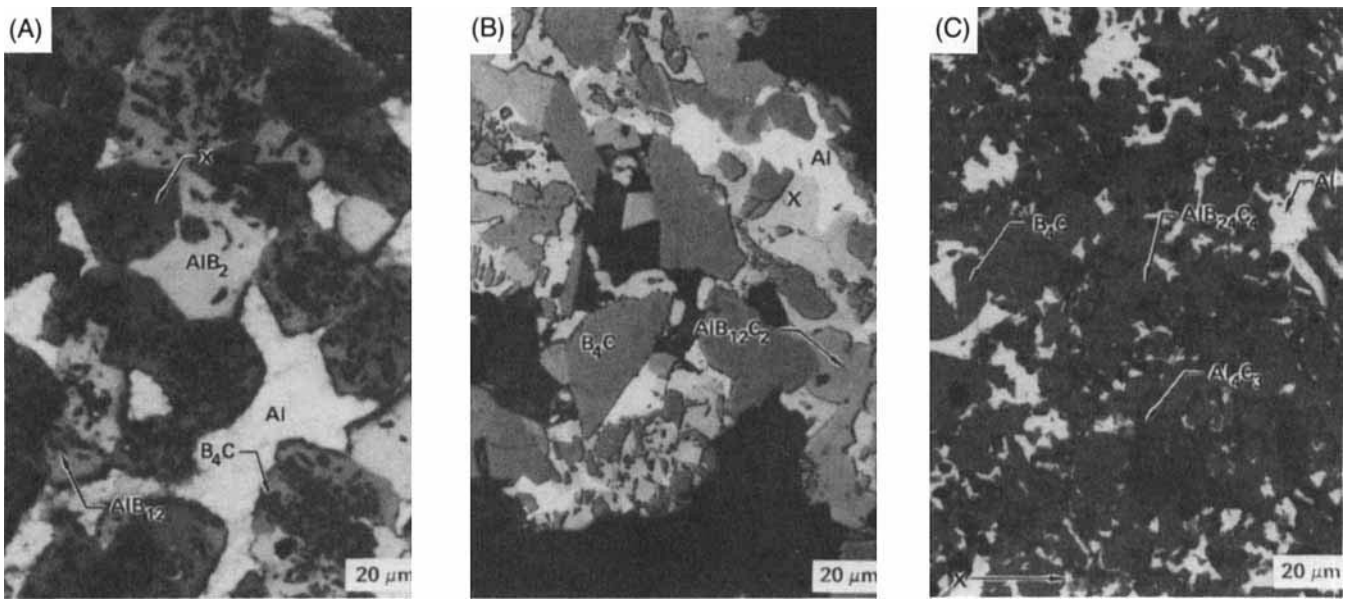

Fig. 3. B_4C–Al cermets showing different sintered microstructures obtained after initially heating to 1180°C for 2 min and subsequently heat-treating at (A) 800°C for 24 h (initial composition: 80 vol% B_4C–20 vol% Al); (B) 1000°C for 1.5 h (initial composition: 70 vol% B_4C–30 vol% Al); and (C) 1300°C for 1 h (initial composition: 30 vol% B_4C–70 vol% Al).

at 800° to 900°C. Small grains (1 to 5 μm) of B_4C are surrounded by large, forming ceramic phases. After 24 h of heat treatment at 800°C (Fig. 3(A)), there is more phase X and AlB_2 than B_4C (initial composition: 80 vol% B_4C–20 vol% Al). This microstructure reaches local equilibrium between phase X, AlB_2, and B_4C within tens of hours at 800°C. After 250 h, the amount of AlB_2 has decreased to form AlB_{12}; after 500 h, B_4C, phase X, AlB_2, $AlB_{12}C_2$, and Al_4C_3 are substantially present in the microstructure. Further heat treatment indicates a tendency to the rapid depletion of phase X and an increase of AlB_{12} and Al_4C_3.

The hypothetical compatibility triangle shown in the lower left-hand corner of Fig. 2 illustrates the tendency toward overall thermodynamic equilibrium. It is assumed that overall equilibrium is achieved when AlB_{12}, Al_4C_3, and B_4C coexist as stable phases.

Above 900°C, but below 1200°C, the following microstructural differences occur: (1) $AlB_{12}C_2$ is thermodynamically favored over AlB_{12} between 900° and 1000°C, and (2) AlB_2 continues to form up to 1000°C; however, above 1000°C, AlB_2 is only present when the microstructure is cooled. Figure 3(B) shows a microstructure resulting from these local equilibrium conditions after 1.5 h at 1000°C (initial composition: 70 vol% B_4C–30 vol% Al).

Between 1200° and 1400°C, the following further changes in the microstructure occur: (1) Al_4C_3 is forming very quickly (associated with a decrease of the ternary phase X); (2) $AlB_{24}C_4$ is now favored over $AlB_{12}C_2$ and becomes the major ternary phase; (3) above 1300°C, XRD patterns indicate the appearance of a phase previously reported as $Al_4B_{1-3}C_4$,[17] but more recently reported as $Al_8B_4C_7$;[28] and (4) at 1400°C, Al_4C_3 begins to crystallize in the shape of short whiskers. Figure 3(C) shows a microstructure characteristic of the local equilibrium conditions after 1 h at 1300°C (initial composition: 30 vol% B_4C–70 vol% Al).

At temperatures above 1300°C, overall equilibrium occurs only after all aluminum and phase X are completely depleted from the system. This is followed by the decomposition of Al_4C_3 and the eventual coexistence of graphite, B_4C, and $AlB_{24}C_4$ as the remaining stable phases. The compatibility triangle in the lower right-hand corner of Fig. 2 illustrates this global equilibrium condition.

Our reaction thermodynamic study determined that local equilibrium conditions between 800° and 1200°C must be established so that phase X will evolve and consequently tie up most of the free carbon required to form Al_4C_3. Because of its hygroscopic nature and poor mechanical properties, Al_4C_3 is undesirable. Above 1200°C, local equilibrium conditions do not suppress Al_4C_3 formation; however, composites with Al_4C_3 whiskers are more chemically stable because of a protective layer of phase X around them. Therefore, to process B_4C–Al cermets, it is necessary to rapidly heat the composition to near 1200°C to ensure that wetting occurs and subsequently heat-treat these compositions at temperatures below 1200°C if further microstructural development is desired.

(3) Densification Kinetics

Fully dense states can be achieved prior to reaching desired thermodynamic conditions either by slowing down reaction kinetics or by speeding up densification kinetics. Favorable results can be obtained by employing small-size powders; however, in our study, the larger B_4C powders (56 μm) were primarily used for two reasons. First, because appropriate colloidal processing techniques for codispersing B_4C and aluminum powders had not yet been developed, the 4- and 10-μm B_4C powders resulted in large agglomerates (250 μm) which led to microstructural inhomogeneities during sintering. Second, we wanted to show that B_4C–Al composites could be fabricated without agglomeration problems and at the same time reduce the rate of chemical reactions by decreasing the B_4C–Al interfacial area.

The starting B_4C particle size did not affect the cold-pressed B_4C–Al green density. All three particle sizes result in producing ≈65% dense green parts with 30 vol% aluminum content and ≈72% dense green parts with 50 vol% aluminum content.

B_4C–aluminum compacts will undergo neither pressureless nor pressure-assisted densification unless wetting occurs. Our pressureless sintered compacts always had residual porosity from 28 vol% (for compacts containing 30 to 45 vol% aluminum) to as high as 44 vol% (for compacts containing 15 to 30 vol% aluminum). This occurred despite the fact that conditions for wetting were obtained; however, compacts with larger B_4C particles (56 μm) did achieve slightly higher densities than compacts with smaller B_4C particles (4 and 10 μm). In all cases, compact sintered densities were about 5% lower than their initial green densities. Even when pressure techniques (vacuum hot-pressing and hot isostatic pressing) were applied to compacts containing between 15 and 60 vol% aluminum, porosity was not completely eliminated, although it was significantly reduced.

High levels of porosity in the pressureless-sintered compacts occurred because (1) at temperatures required for densification (wetting), chemical reaction rates are faster than the spreading

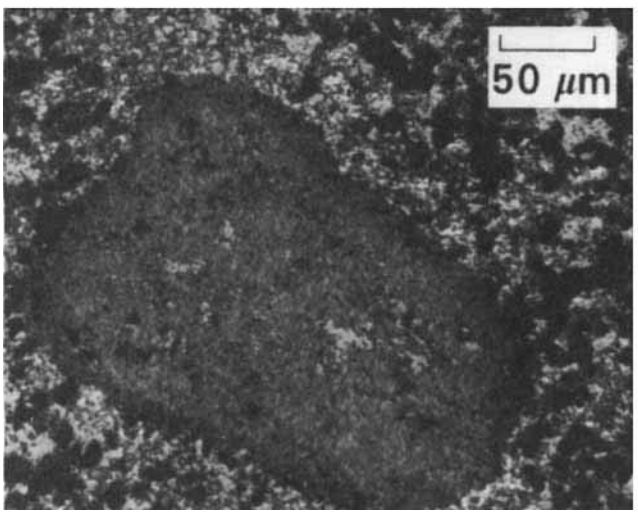

Fig. 4. B_4C–Al (30 vol%) cermet hot-pressed at 1180°C under vacuum (5×10^{-2} Pa) for 6 min at 15 MPa (≈2000 psi) showing a region of local densification surrounded by porous regions.

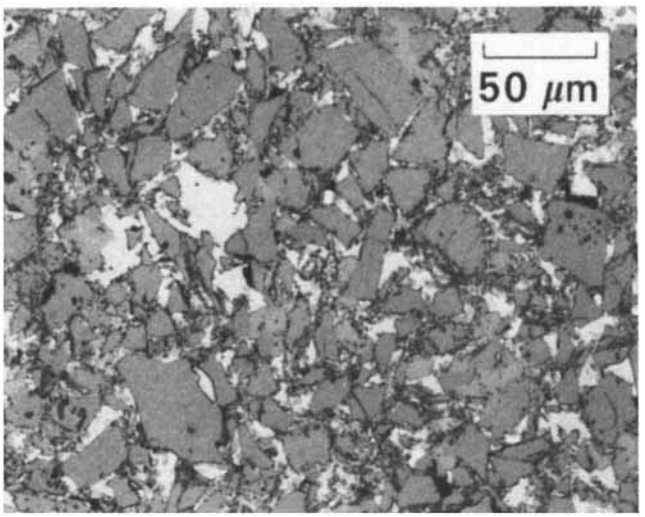

Fig. 5. B_4C–Al (30 vol%) cermet initially sintered at 1180°C for 2 min under vacuum (10^{-3} Pa) and subsequently hot isostatically pressed at 1000°C for 30 min at 207-MPa (≈30 000-psi) argon. Note improvement in uniformity compared with Fig. 4.

Table III. Processing Trade-offs for B_4C–Al Cermets

Processing trade-off	Parameters that control trade-off	Effect of trade-off on reactive-liquid sintering mechanism	Optimum processing
Wetting versus evaporation	High temperature versus low temperature	Depletion of liquid aluminum by evaporation	Use high temperatures for short times
Chemical reaction versus densification	Short time versus long time	Chemical reaction kinetics faster than densification kinetics results in inhibiting rearrangement and depletion of aluminum due to new phase formation	Speed up densification rate by applying pressure and/or slow down chemical reaction rate by increasing B_4C grain size
Axial pressure versus isostatic pressure	Hot-pressing versus hot isostatic pressing	Stress gradients inhibit rearrangement	Hot isostatic pressed presintered compacts

rates for aluminum, and (2) at these temperatures, the vapor pressure for aluminum is higher than that of the vacuum-processing environment employed. Both of these mechanisms result in the depletion of aluminum. The formation of new phases (reaction kinetics), however, has the most detrimental effect. When enough reaction product has formed, the microstructure becomes "locked up," prohibiting further rearrangement. This, combined with the fact that there is an insufficient amount of molten aluminum to fill the remaining pores, results in high-porosity final products.

Table I shows the results of the vacuum-hot-pressed compacts. These results indicate that increasing the aluminum content does reduce the amount of porosity in the cermet. Also, increasing the pressure (while lowering the hot-pressing temperature to slow down the depletion of aluminum) reduced, but did not eliminate, porosity completely.

Densification by hot-pressing is inhibited by mechanisms other than the competition between phase formation and the capillary flow of molten aluminum. Figure 4 shows regions where local densification is obtained by satisfying the capillarity–thermodynamic criterion of low contact angles, while grossly porous regions are sporadically located adjacent to these dense regions. Agglomeration of the B_4C particles will also increase this effect.

Axial forces applied to powders during vacuum hot-pressing in a graphite die result in radial forces on the compact. The magnitude of these radial forces is largely dependent on the plasticity of the powders and always results in stress-concentration gradients within the compact.[33] When B_4C grains are forced to bridge or lock tightly in regions of high-stress concentrations, liquid rearrangement by capillary action will be hindered. This will permit local densification where rearrangement is possible (low-stress concentration areas within the compact), resulting in aluminum-depleted regions where bridging is the strongest.

Since we desired to achieve densification without depleting aluminum and also avoid the previously described mechanisms inhibiting uniform rearrangement, we hot isostatic pressed presintered compacts. (The presintered compacts were sealed under vacuum in stainless-steel cans.)

Table II shows the results of the hot isostatic pressed compacts. Even with hot isostatic pressing, however, the results indicate that a minimum amount of aluminum is required to reduce porosity to negligible levels ($\leq$1.0 vol%). Hot isostatic pressed, presintered compacts had connected porosities $\leq$3.5 vol%, whereas nonpresintered (nonwetted) compacts had porosities in excess of 10 vol%. As aluminum content was increased above 30 vol%, connected porosities dropped to below 1 vol%. A hot isostatic pressed microstructure is shown in Fig. 5. The microstructure confirms that the uniform application of pressure resulted in (1) accelerating the densification kinetics faster than the chemical reaction kinetics and (2) elimination of stress-induced microstructural inhomogeneities.

Our study has shown that certain processing trade-offs must be considered to produce B_4C–Al composites. Table III summarizes these trade-offs.

IV. Conclusions

Based on fundamental capillarity thermodynamics, reaction thermodynamics, and densification kinetics, definite processing criteria have been established for obtaining B_4C–Al composites. In these materials, chemical reactions occur between 800° and 1400°C. These interfacial reactions are the driving force for the wetting of B_4C by molten aluminum. Because the chemical reactions cannot be eliminated, it is necessary to process B_4C–Al by rapidly heating to near 1200°C (to ensure wetting) and subsequently heat-treating below 1200°C (for microstructural development). Densification is inhibited because chemical reactions occur faster than capillarity-induced liquid rearrangement. Therefore, it is necessary to apply pressure to accelerate densification faster than the kinetics of phase formation, which is the major hindrance to rearrangement during pressureless sintering. To ensure microstructural homogeneity, it is also necessary to apply this pressure in a uniform manner by hot isostatic pressing presintered compacts.

References

[1] A. Lipp, "Boron Carbide: Production, Properties, Applications" (in Ger.), *Tech. Rundsch.*, **57** [14] 5 (1965); **57** [28] 14 (1965); **57** [33] 3 (1965); **58** [7] 3 (1966).

[2] G. de With, "High-Temperature Fracture of Boron Carbide: Experiments and Simple Theoretical Models," *J. Mater. Sci.*, **19**, 457–66 (1984).

[3] S. Prochazka and S. L. Dole, "Development of Spacecraft Materials and Structures Fundamentals," Rept. No. SRD–85–021, General Electric Company Corporate Research and Development, Schenectady, NY, 1985.

[4] M. Beauvy and R. Angers, "Mechanisms of Hot-Pressing of Boron Carbide Powders"; pp. 279–86 in Science of Ceramics, Vol. 10. Edited by H. Hausner. Deutsche Keramische Gesellschaft, Weiden, FRG, 1980.

[5] J. A. Cornie, R. Suplinskas, and A. Hauze, "Boron–Aluminum Composites"; p. 28 in Proceedings of Advanced Fibers and Composites for Elevated Temperatures. Edited by I. Ahmad and B. R. Noton. The Metallurgical Society of AIME, Warrendale, PA, 1980.

[6] S. D. Karmarkar and A. P. Divecha, "Fabrication and Properties of Boron Carbide–Reinforced Aluminum Composites," NSWC TR 84-160, Naval Surface Weapons Center, Dahlgren, VA, 1984.

[7] P. R. Roy and C. Ganguly, "Dispersion-Type Composites for Nuclear Reactors"; pp. 159–79 in Sintered Metal–Ceramic Composites. Edited by G. S. Upadhaya. Elsevier, Amsterdam, Netherlands, 1984.

[8] J. E. Smugeresky, H. J. Rack, and G. B. Brasell, "Development of a Non-Volatile Boron Carbide–Copper Cermet Neutron Shield for High-Performance Shipping Casks," SAND–80–0802C, Sandia National Laboratories, Alburquerque, NM, 1981.

[9] I. A. Aksay, C. E. Hoge, and J. A. Pask, "Wetting under Chemical Equilibrium and Nonequilibrium Conditions," *J. Phys. Chem.*, **78**, 1178–83 (1974).

[10] C. R. Manning and T. B. Gurganus, "Wetting of Binary Aluminum Alloys in Contact with Be, B_4C, and Graphite," *J. Am. Ceram. Soc.*, **52** [3] 115–18 (1969).

[11] A. D. Panasyuk and T. V. Dubovik, "Wetting of Boron Carbide System Samples with Molten Metals" (in Russ.), *Dielektriki (Dieletr. Poluprovodn.)*, **2**, 120–25 (1972).

[12] G. A. Kolesnichenko, "Wettability of Refractory Covalent Crystals by Metallic Melts" (in Russ.), *Smachivaemost Poverkn. Svoistva Rasplavov Tverd. Tel. 1972*, 71–74.

[13] A. D. Panasyuk, V. D. Oreshkin, and V. R. Maslennikova, "Kinetics of the Reactions of Boron Carbide with Liquid Aluminum, Silicon, Nickel, and Iron," *Sov. Powder Metall. Met. Ceram. (Engl. Transl.)*, **18** [7] 487–90 (1979).

[14] A. D. Panasyuk, V. R. Maslennikova, and E. V. Marek, "Reactions of Materials of the B_4C–Cr System with Liquid Metals," *Sov. Powder Metall. Met. Ceram. (Engl. Transl.)*, **20** [10] 729–32 (1982).

[15] M. W. Lindley and G. E. Gazza, "Some New Potential Ceramic–Metal Armor

Materials Fabricated by Liquid Metal Infiltration," AD-769742, Army Materials and Mechanics Research Center, Watertown, MA, 1973.
[16]J. A. Kohn, G. Katz, and A. A. Giardini, "AlB_{10}, a New Phase, and a Critique on Aluminum Borides," *Z. Kristallogr.*, **111**, 53–62 (1958).
[17]V. I. Matkovich, J. Economy, and R. F. Giese, Jr., "Presence of Carbon in Aluminum Borides," *J. Am. Chem. Soc.*, **86**, 2337–40 (1964).
[18]V. I. Matkovich, R. F. Giese, Jr., and J. Economy, "Phases and Twinning in $C_2Al_3B_{48}$ (beta AlB_{12})," *Z. Kristallogr.*, **122**, 108–15 (1965).
[19]A. Lipp and M. Röder, "On the Subject of Aluminum-Containing Boron Carbides" (in Ger.), *Z. Anorg. Allg. Chem.*, **343**, 1–5 (1966) (translated by Leo Kanner Associates, Redwood City, CA, 1971).
[20]R. F. Giese, Jr., J. Economy, and V. I. Matkovich, "Topotactic Transition in C_4AlB_{24}," *Acta Crystallogr.*, **20**, 697–98 (1966).
[21]G. Bliznakov, P. Peshev, and T. Niemyski, "On the Preparation of Crystalline Aluminum Borides by a Vapour Deposition Process," *J. Less-Common Met.*, **12**, 405–10 (1967).
[22]E. L. Muetterties, The Chemistry of Boron and Its Compounds; pp. 84–90. Wiley, New York, 1967.
[23]G. Will, "The Crystal Structure of C_4AlB_{24}," *Acta Crystallogr., Sect. B: Struct. Crystallogr. Cryst. Chem.*, **B25**, 1219–22 (1969) (translated by Lawrence Livermore National Laboratory, Livermore, CA, UCRL TRANS-11966, 1984).
[24]A. J. Perrotta, W. D. Townes, and J. A. Potenza, "Crystal Structure of $C_8Al_{2.1}B_{51}$," *Acta Crystallogr., Sect. B: Struct. Crystallogr. Cryst. Chem.*, **B25**, 1223–29 (1969).
[25]H. Neidhard, R. Mattes, and H. Becher, "The Production and Structure of a Boron Carbide Containing Aluminum," *Acta Crystallogr., Sect. B: Struct. Crystallogr. Cryst. Chem.*, **B26**, 315–17 (1970) (translated by Lawrence Livermore National Laboratory, Livermore, CA, UCRL TRANS-11965, 1984).
[26]G. Will, "On the Existence of AlB_{10}: A Critical Review of the Crystal Structures of AlB_{10} and C_4AlB_{24}," *Electron Technol.*, **3**, 119–26 (1970).
[27]G. V. Samsonov, V. A. Neronov, and L. K. Lamikhov, "The Conditions, Structure, and Some Properties of Phases in the Al–B System," *J. Less-Common Met.*, **67**, 291–96 (1979).
[28]Z. Inouhe, H. Tanaka, and Y. Inomata, "Synthesis and X-ray Crystallography of Aluminum Boron Carbide, $Al_8B_4C_7$," *J. Mater. Sci.*, **15**, 3036–40 (1980).
[29]M. L. Wilkins, C. F. Cline, and C. A. Honodel, "Light Armor," UCRL-71817, Lawrence Livermore National Laboratory, Livermore, CA, 1969.
[30]Powder Diffraction File, Card No. Joint Committee on Powder Diffraction Standards, Swarthmore, PA, 1985.
[31]D. C. Halverson, A. J. Pyzik, and I. A. Aksay, "Boron-Carbide-Aluminum and Boron-Carbide-Reactive Metal Cermets," U.S. Pat. No. 4 605 440, Aug. 12, 1986.
[32]M. Sarikaya, T. Laoui, D. L. Milius, and I. A. Aksay, "Identification of a New Phase in the Al-B-C Ternary By High-Resolution Transmission Electron Microscopy"; pp. 168–69 in Proceedings of the 45th Annual Meeting of the Electron Microscopy Society of America. Edited by G. W. Bailey. San Francisco Press, San Francisco, CA, 1987.
[33]R. A. Thompson, "Mechanics of Powder Pressing: I, II, III," *Am. Ceram. Soc. Bull.*, **60**, [2] 237–51 (1981). □

journal

J. Am. Ceram. Soc., **72** [5] 780–84 (1989)

Electrochemical Techniques for Corrosion Rate Determination in Ceramics

Ramesh Divakar,* Srinvasa G. Seshadri,* and Makuteswara Srinivasan*

Technology Division, Standard Oil Engineered Materials Company, Niagara Falls, New York 14302

Standard electrochemical test procedures have been successfully applied to determine the corrosion rates of SiC-based ceramics in aqueous reagents. Direct-current polarization measurements in HCl solutions indicate that the corrosion rate of α-SiC is 0.0050 ± 0.0002 mil/yr and is fairly independent of HCl concentration. The corrosion rates of α-SiC are significantly lower than those for reaction-sintered SiC in all of the electrolytes used including HCl, HNO_3, H_3PO_4, and aqua regia. It is believed that the free Si contained in the reaction-sintered SiC is responsible for the higher corrosion rates. It has been shown that electrochemical techniques are reproducible and eminently suitable for determining very low corrosion rates encountered in ceramics. [Key words: silicon carbide, electrochemistry, corrosion, electrical properties, polarization.]

I. Introduction

A COMMON application of the high-performance ceramics, such as silicon carbide, is in the chemical processing industry where acids, alkali, and other combinations of corrosive fluids are pumped, requiring corrosion and wear-resistant seals.[1] Although the corrosion rates of ceramics are generally small compared to the metallic components, the corrosion behavior of potential seal materials is not well documented in various reagents or combinations of liquids that may be encountered in service.

In the past, the corrosion rates of ceramics have been determined mostly by periodic weight loss measurements after immersion in the electrolyte of interest, but the applicability of this method to extremely low corrosive conditions is very limited. Furthermore, prolonged test periods are needed (over 200 h) for reasonable accuracy in weight loss measurements. Therefore, the development of a comprehensive data base on corrosion rates of various ceramics in different reagents at temperatures of interest is a laborious task. This technique, however, is simple and straightforward and does not require any knowledge of corrosion reactions that are occurring.

The electrochemical techniques, on the other hand, offer a potentially easier and quicker way to determine the corrosion rates. The basis for this approach lies in the implicit understanding of the chemical reactions that are responsible for corrosion. In addition, appropriate electrochemical theories and analysis procedures need to be developed to reduce the current and voltage observations to corrosion rate information. Many different procedures utilizing dc and ac techniques have been evolved in recent years,[2–5] each providing a wealth of information on the corrosion phenomena for metals and alloys. With improved instrumentation and analysis, these methods have become very practical.

A survey of the corrosion literature reveals that, except for a cursory study,[6] there has been very little work done in the area of electrochemical corrosion of ceramics. In this work, an attempt is made to evaluate the applicability of these techniques to two SiC-based ceramics in various aqueous reagents. This work is also aimed at the development of electrochemical test procedures for ceramics and ceramic composites since no standards are available

J. L. Smialek—contributing editor

Manuscript No. 199103. Received June 6, 1988; approved October 4, 1988.
Presented at the 89th Annual Meeting of the American Ceramic Society, Pittsburgh, PA (Engineering Ceramics Division, Paper No. 62-C-87).
*Member, American Ceramic Society.